Research on High Frequency Vibration Reduction Using Carrier Phase Shifted PWM for 4-module 3-Phase Permanent Magnet Synchronous Motor

Zicheng Liu *Member, IEEE,* She Yan, Haiyang Fang *Member, IEEE,*

Dong Jiang *Senior Member, IEEE*, Ronghai Qu *Fellow, IEEE*

***Abstract*—This paper investigates the effect of the Carrier Phase Shifted Pulse Width Modulation (CPS-PWM) on the vibration reduction of inverter-fed multi-phase permanent magnet synchronous motors(PMSMs). This approach reduces vibration by changing the order of the carrier harmonic-induced electromagnetic force on the stator. Experiments verify that this method can effectively suppress vibration at a specific carrier frequency, but the vibration reduction effect depends on the carrier frequency, the modal frequency of the motor and the phase-shifted angles.**

***Index Terms*—Multi-phase motor, permanent magnet synchronous motor, Carrier Phase Shifted Pulse Width Modulation, high-frequency electromagnetic vibration**

I. INTRODUCTION

Multiphase PMSMs fed by converters are widely used in energy conversion areas requiring high reliability like electric propulsion applications, due to the excellent fault tolerance capability[1-4]. However, when the converter is working under PWM, high-frequency harmonic currents are introduced into the stator windings, resulting in high-frequency(HF) electromagnetic(EM) force, and HF vibration, which destroys the stealth performance of the propulsion system.

In order to reduce the high frequency EM vibration introduced by the converter, many scholars have carried out research work from the perspective of changing the carrier frequency. Literature [5] pointed out that if the carrier frequency avoids the natural frequency of the motor, HF vibration would be obviously reduced. But for different motors, it is very difficult to select an appropriate carrier frequency. Literature [6] proposed a variable carrier frequency PWM strategy based on the rotor position, which broadened the spectrum of harmonic currents to reduce the peak values of HF harmonic currents, and therefore could suppress the HF vibration. However, because these methods usually lack accurate analysis of the motor vibration response, the variable carrier frequency may sometimes worsen the HF vibration [7].

Some scholars have also explored how to reduce HF vibration at a fixed carrier frequency. For dual three-phase motors powered by parallel inverters, a PWM method with a carrier phase shift of 90 degrees is proposed in reference [8], which leads to opposite phases of the harmonics at two times the carrier frequency in the two sets of three-phase windings opposite, and effectively reduces HF vibration acceleration. Literature [9] sets a 180-degree phase shift on the carrier of the dual three-phase inverter, so that the phases of current harmonic at odd multiples of the carrier frequency in the two sets of three-phase windings are opposite, which also reduces the HF vibration of the motor.

However, the above methods all rely on the cancellation of HF components in the magnetomotive force generated by the dual three-phase windings. This requires special designs such as common slots or interval slots for the dual three-phase windings of the motor, which severely limits the methods when extended to other types of motors.

In short, existing researches usually focus on the frequency and magnitude of EM force, ignoring the influence of the spatial order of EM force on vibration. There lacks research on vibration reduction by adjusting the order of EM force.

This paper proposes a carrier phase shifted method for 4*3-phase PMSMs. The order of EM force is adjusted by carrier phase shift to suppress vibration. Firstly, the 4-module 3-phase PMSM and its drive system are introduced, along with the analysis of the EM force. Then the vibration reduction mechanism of CPS-PWM is illustrated, considering the orders of HF EM forces. Finally, experimental results confirm with the theory analysis of EM force effects on vibration, and demonstrate that the proposed CPS-PWM can significantly reduce HF vibration under certain conditions.

II. THE MODEL OF 4-MODULE 3-PHASE PMSM

Fig. 1 shows the structure of the 4- module 3-phase PMSM. The motor has four sets of windings which are arranged in four sectors along the stator. So the mutual inductance among different sets of windings is small. The electrical angles of different sets of windings differ by 0 °.

Fig. 2 shows the 4-module PMSM drive system. The system consists of four sets of three-phase voltage source

This work was supported in part by the National Science and Foundation of China under Grant 52077088. *(Corresponding author: Haiyang Fang)*

inverters(VSIs) to drive the 4-module PMSM. Each set of the three-phase motor windings is fed by a three-phase VSI module. Therefore, each set of three-phase stator currents can be independently controlled. As a result, the number of switching devices required is 4 times that of the traditional three-phase motor drive system, and the hardware cost is increased.

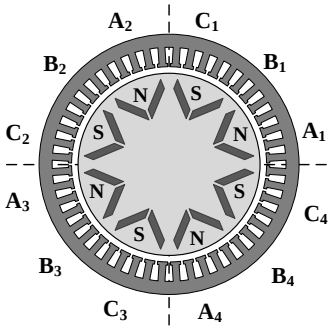

Fig. 1. Structure of the 4-module 3-phase PMSM

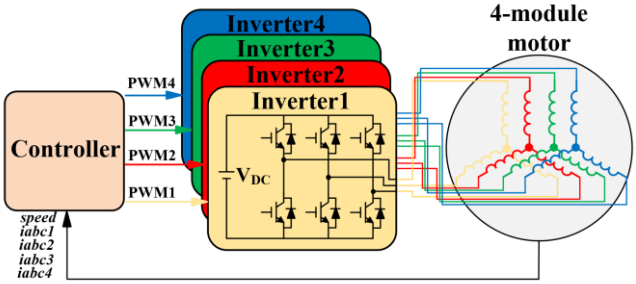

Fig.2. Schematic of 4-module PMSM drive system

III. Analysis of High-frequency Electromagnetic Force of PMSM

The HF EM vibration of the motor is mainly generated by the HF EM force acting on the stator [10]. For PMSM, the HF EM force induced by PWM can be expressed as [11]

$$f_{pwm}(\theta,t)=\sum_{\nu}\sum_{\omega} f_{\nu,\omega}\cos(\nu\theta-\omega t+\varphi) \tag{1}$$

$$\nu=0,2p \tag{2}$$

$$\omega=m\omega_c\pm n\omega_o\,(m\geq 1,n\geq 0) \tag{3}$$

$$\varphi=m\theta_c\pm n\theta_o \tag{4}$$

where ν , ω and φ stand for the spatial order, angular frequency and phase of the EM force, respectively. p is the pole pairs number of the motor. ω_c and ω_o are the angular frequencies of the carrier and modulation wave, respectively. m, n are the index coefficient of the carrier and modulation wave. θ_c and θ_o are the phase of the carrier and modulation wave, respectively.

Formula (2) shows the spatial distribution of the EM force. It should be noted that the Formula (2) only applies to integer slot motors. For fractional slot motors, the spatial order of the HF EM force is very complex, which needs to be analyzed in combination with the specific motor structure.

Formula (3) shows the frequency characteristics of HF EM force under the Sinusoidal PWM(SPWM). All the HF harmonics concentrated around integral multiples of the carrier frequency. In Formula (3),when m is odd, n is $1,3,5,7,9\ldots$. When m is even, n is $0,2,4,6,8\ldots$. So it can also be expressed as

$$\begin{cases}\omega=\omega_c\pm\omega_o,\ \omega_c\pm 3\omega_o,\ldots\\ \omega=2\omega_c,\ 2\omega_c\pm 2\omega_o,\ldots\\ \ldots\ldots\end{cases} \tag{5}$$

Formula (4) shows the phase characteristics of HF EM force. It can be seen from Formula (4) that the phase of the EM force can be changed by changing the phase of the carrier. The phase of the carrier changes X, the phase of EM force at m times the carrier frequency(mf_c) changes mX.

IV. The Mechanism of Vibration Generation and Reduction

A. *Theoretical Analysis Vibration Generation*

Fig. 3 shows a typical mechanical transfer function curve of the motors, which can be obtained by modal experiment or finite element simulation. Decomposing the mechanical transfer function, the mechanical transfer function curve of each order modal can be obtained, as shown in Fig. 4.

The ν -order transfer function in Fig. 4 can be expressed as

$$H(\nu,\omega)=\frac{1}{\left[\left(\frac{\omega}{\omega_\nu}\right)^2-1\right]+2\zeta_\nu\frac{\omega}{\omega_\nu}i}=\left|H(\nu,\omega)\right|e^{j\theta_{\nu,w}} \tag{6}$$

$$\left|H(\nu,\omega)\right|=\frac{1}{\sqrt{\left[(\frac{\omega}{\omega_\nu})^2-1\right]^2+(2\zeta_\nu\frac{\omega}{\omega_\nu})^2}} \tag{7}$$

where ω_ν and ζ_ν are the natural frequency and damping ratio of the ν -order modal, respectively. Obviously the overall mechanical transfer function in Fig. 3 can be expressed as $\sum_{\nu}H(\nu,\omega)$.

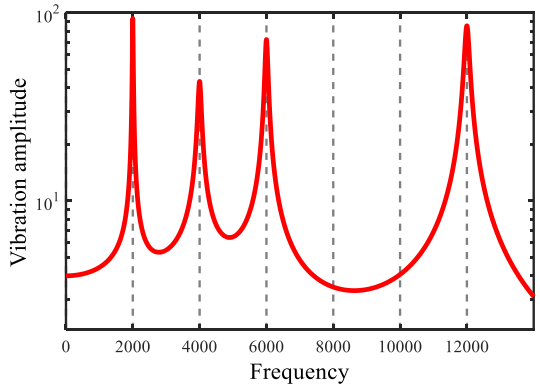

Fig. 3. Overall mechanical transfer function curve

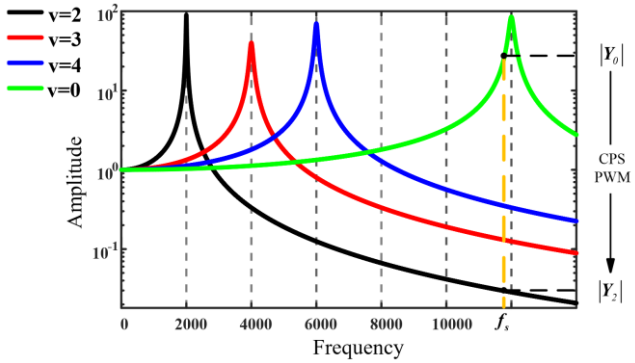

Fig. 4. Decomposed mechanical transfer function

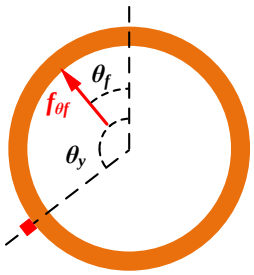

Fig. 5. Schematic diagram of the forces on the stator

In order to simplify the analysis, the motor stator is simplified as a ring, as shown in Fig. 5.

From Formula (1), it can be known that the μ -order HF EM force density can be expressed as

$$f_\mu = f_{m\mu}\cos(\mu\theta - \omega t + \varphi_\mu) \tag{8}$$

As shown in Fig. 5, the EM force at point θ_f is expressed as

$$f_{\theta_f} = f_{m\mu}\cos(\mu\theta_f - \omega t + \varphi_\mu)\mathrm{d}\theta_f \tag{9}$$

The vibration response at point θ_y is

$$\begin{aligned} y &= f_{\theta_f} \times \sum_v H(v,\omega) \\ &= f_{m\mu}\cos(\mu\theta_f - \omega t + \varphi_\mu)\mathrm{d}\theta_f \times \sum_v H(v,\omega) \\ &= \sum_v f_{m\mu}\left|H(v,\omega)\right|\cos\left[\mu\theta_f + v(\theta_y - \theta_f) - \omega t + \varphi_{u,v,\omega}\right]\mathrm{d}\theta_f \end{aligned} \tag{10}$$

The vibration response produced by the total μ -order EM force at point θ_y is

$$\begin{aligned} Y &= \int_0^{2\pi}\sum_v f_{m\mu}\left|H(v,\omega)\right|\cos\left[\mu\theta_f + v(\theta_y - \theta_f) - \omega t + \varphi_{u,v,\omega}\right]\mathrm{d}\theta_f \\ &= \sum_v f_{m\mu}\left|H(v,\omega)\right|\int_0^{2\pi}\cos\left[\mu\theta_f + v(\theta_y - \theta_f) - \omega t + \varphi_{u,v,\omega}\right]\mathrm{d}\theta_f \end{aligned} \tag{11}$$

when $\mu \neq v$,

$$\begin{aligned} &f_{m\mu}\left|H(v,\omega)\right|\int_0^{2\pi}\cos\left[\mu\theta_f + v(\theta_y - \theta_f) - \omega t + \varphi_{u,v,\omega}\right]\mathrm{d}\theta_f \\ &= f_{m\mu}\left|H(v,\omega)\right|\int_0^{2\pi}\cos\left[(\mu - v)\theta_f + v\theta_y - \omega t + \varphi_{u,v,\omega}\right]\mathrm{d}\theta_f \\ &= f_{m\mu}\left|H(v,\omega)\right|\times 0 \\ &= 0 \end{aligned} \tag{12}$$

That is, the v -order modal can only be excited by the same order of EM force to generate corresponding vibration [12].

Therefore, Formula (11) can be simplified as

$$\begin{aligned} Y &= f_{m\mu}\left|H(\mu,\omega)\right|\int_0^{2\pi}\cos\left[\mu\theta_f + \mu(\theta_y - \theta_f) - \omega t + \varphi_{\mu,v,\omega}\right]\mathrm{d}\theta_f \\ &= 2\pi f_{m\mu}\left|H(\mu,\omega)\right|\cos(\mu\theta_y - \omega t + \varphi_{\mu,v,\omega}) \end{aligned} \tag{13}$$

The EM force with multiple spatial orders can be expressed as

$$\begin{aligned} F &= \sum_\mu f_\mu \\ &= \sum_\mu f_{m\mu}\cos(\mu\theta - \omega t + \varphi_\mu) \end{aligned} \tag{14}$$

Combined with Formula (13), the vibration it generates at point θ_y can be expressed as

$$\begin{aligned} Y &= \sum_\mu 2\pi f_{m\mu}\left|H(\mu,\omega)\right|\cos(\mu\theta_y - \omega t + \varphi_{\mu,v,\omega}) \\ &= \sum_\mu \left|Y_\mu\right|\cos(\mu\theta_y - \omega t + \varphi_{\mu,v,\omega}) \end{aligned} \tag{15}$$

$$\left|Y_\mu\right| = 2\pi f_{m\mu}\left|H(\mu,\omega)\right| \tag{16}$$

B. The Mechanism of Vibration Reduction

From the above analysis we can draw the following conclusions:

(1) The electromagnetic force can only act with the same order modal or the same order transfer function to excite vibration.

(2) For the integer slot motor we studied, the high-frequency EM force in the motor is dominated by 0-order.

(3) When the electromagnetic force order is close to the natural frequency of a certain order modal, the effect of this order modal is much greater than that of other orders, as shown in Fig. 4. Which can be expressed by

$$\left|H(\mu,\omega_s)\right| \gg \left|H(v,\omega_s)\right| \qquad \mu \neq v \quad \omega_s \approx \omega_{n\mu} \tag{17}$$

For the high-frequency EM force in the integer motor, its spatial order is 0, and it only interacts with 0-order modal or 0-order transfer function to generate vibration. The vibration amplitude it produces is

$$\left|Y_0\right| = 2\pi f_m\left|H(0,\omega_s)\right| \tag{18}$$

where ω_s and f_m is the angular frequency and amplitude of the EM force.

If the order of the EM force is changed from 0 to 2 without changing its amplitude and frequency, then it only interacts with 2-order modal or 2-order transfer function to generate vibration. In this condition, the vibration amplitude generated by it is

$$\left|Y_2\right| = 2\pi f_m\left|H(2,\omega_s)\right| \tag{19}$$

When the EM force frequency ω_s is close to the 0-order modal natural frequency ω_{n0} , from conclusion (3) it can be seen that

$$\begin{aligned} \left|H(0,\omega_s)\right| &\gg \left|H(2,\omega_s)\right| \\ 2\pi f_m\left|H(0,\omega_s)\right| &\gg 2\pi f_m\left|H(2,\omega_s)\right| \end{aligned} \tag{20}$$

Comparing the vibrations generated by the EM force before and after changing the its order, we can obtain the following expression

$$|Y_0| \gg |Y_2| \tag{21}$$

That is, by changing the order of the EM force, the vibration generated by it would be greatly reduced, as shown in Fig. 4.

V. Carrier Phase Shifted PWM and Vibration Redution

A. *How Carrier Phase Shifted PWM Changes the Order of the Electromagnetic Force*

It can be seen from Chapter 1 that each module of the 4-module 3-phase motor is independent of each other, so the EM force generated by each module can be decoupled. Therefore, by changing the phase of the carrier of each module, the phase of the EM force generated by each module is changed.

As shown in Fig. 6, taking the carrier of the first module as a reference, we can set the carrier phases of the second to fourth module as θ_2 , θ_3 , θ_4 , and record this carrier phase combination(CPC) as 0-θ_2 -θ_3 -θ_4 .

It can be seen from Formula (4) that when the CPC is 0-$\frac{180}{m}$ -0-$\frac{180}{m}$, the phase combination of EM force at around mf_c is 0-180-0-180. At this time, the order of EM force at around mf_c changes from 0 to 2, as shown in Fig. 7.

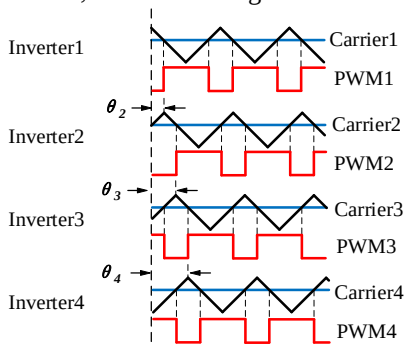

Fig. 6. Schematic diagram of CPS-PWM

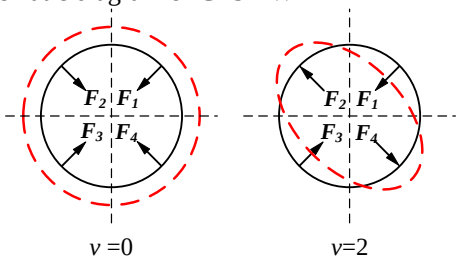

Fig. 7. Change of the order of the EM force

B. *The Relationship between the Electromagnetic Force Order and the Carrier Phase Combination*

It can be seen from Formula (2) that before the CPS-PWM is adopted, the main orders of the electromagnetic force are 0-order and *2p*-order. The higher the order, the smaller the vibration generated by the EM force[13]. Therefore, the *2p*-order electromagnetic force can be ignored, and the electromagnetic force can be regarded as 0-order. So the EM force can be expressed as

$$\begin{aligned} f_{pwm} &= f_m \cos(v\theta - \omega t + \varphi) \\ &= f_m \cos(0\theta - \omega t + m\theta_c \pm n\theta_b + \theta_0) \\ &= f_m \cos(-\omega t + m\theta_c + \theta_{\omega,n,t}) \end{aligned} \tag{22}$$

Next, the order change of the electromagnetic force is mainly analyzed. In order to simplify the analysis, the time variable *t* is ignored. Take $t = t_0$ so that

$$f_{pwm} = f_m \cos(-\omega t_0 + m\theta_c + \theta_{\omega,n,t_0}) = f_m \tag{23}$$

For the EM force with frequency $m\omega_c \pm n\omega_o$, assuming that $-\omega t_0 + m\theta_c + \theta_{\omega,n,t_0} = 0$ when the CPC is 0-*X*-0-*X*, the following expression can be obtained.

$$\begin{cases} f_{pwm} = f_m & \theta \in [0, 90^\circ) \\ f_{pwm} = f_m \cos(mX) & \theta \in [90, 180^\circ) \\ f_{pwm} = f_m & \theta \in [180, 270^\circ) \\ f_{pwm} = f_m \cos(mX) & \theta \in [270, 360^\circ) \end{cases} \tag{24}$$

The amplitude of each order EM force can be obtained by performing fast Fourier transform(FFT) on Formula (24). And Formula (24) can also be expressed as

$$\begin{aligned} f_{pwm} &= f_{m0} + f_{m1}\cos(\theta) + f_{m2}\cos(2\theta) + \dots \\ &= \sum_{\mu} f_{m\mu} \cos(\mu\theta) \end{aligned} \tag{25}$$

Although there are many kinds of CPCs, only two kinds of CPCs are the most helpful for vibration suppression, which are 0-*X*-0-*X* and 0-0-*X*-*X*.

Fig. 8 and Fig. 9 show that when CPC is 0-*X*-0-*X* and 0-0-*X*-*X*, the relative amplitude of each order EM force at around mf_c varies with the carrier phase angle *X*.

As shown in Fig. 8, when the CPS is 0-*X*-0-*X*, the order of the EM force is expressed as $\mu = 0,2,6,10\dots$. The relative amplitude of the 0-order EM force decreases sinusoidally with *X*, and the relative amplitudes of the other-order EM forces increase sinusoidally with *X*. When *X* is $\frac{180^\circ}{m}$, the amplitude of the 0-order EM force is 0 and the 2-order EM force is dominant.

As shown in Fig. 9, when the CPS is 0-0-*X*-*X*, the order of the EM force is expressed as $\mu = 0,1,3,5\dots$. In general, there is no 1-order modal of the motor[14], so the vibration generated by the 1-order EM force can be ignored. Therefore, ignoring the 1-order EM force, it is considered that when the CPA is $\frac{180^\circ}{m}$, the 3-order EM force is dominant.

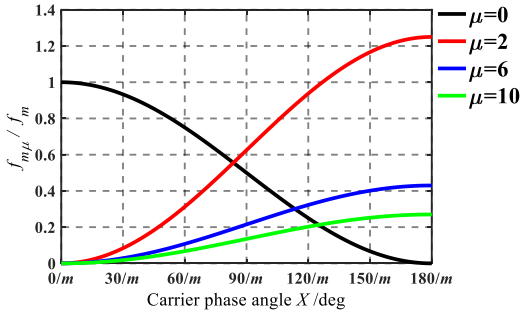

Fig. 8. Change of orders under CPC 0-*X*-0-*X*

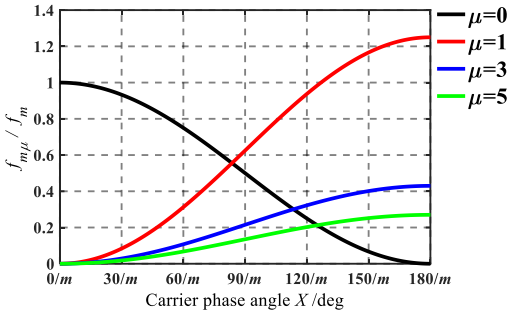

Fig. 9. Change of orders under CPC 0-0-*X*-*X*

VI. Experimental Validation

To verify the above analysis, experiments are conducted on three different PMSMs, which are a 4-module PMSM(motor 1) with 48 slots and 8 poles, a 2-module PMSM(motor 2) with 12 slots and 8 poles, and a 4-module PMSM(motor 3) with 12 slots and 16 poles. The following three groups of experiments are described in details.

A. Introduction to the experimental platform

The structures of the three motors are shown in Fig. 10. The basic parameters are shown in Table I.

As shown in Fig. 11, the modal natural frequencies were obtained by tapping the hanging motors using the testing hammer. The natural frequencies of the three motors are listed in Table II.

The experimental platform is shown in Fig. 12. Accelerometers are evenly arranged on the stator surface. The motors are driven by the inverters to run at a constant speed, and then the vibration acceleration is measured and the vibration spectrum can be obtained. The average of the vibration amplitudes measured by all sensors is taken as the vibration index of the experiment result. To verify the effects of CPS-PWM, we change the carrier frequency and CPCs, and then compare the vibration results under different conditions.

The harmonic current at around $2f_c$ generated by the VSIs is the largest[15], so the vibration at around $2f_c$ is generally the largest. Therefore, we focus on the change of the vibration at around $2f_c$. It can be seen from formula (4) that for any value of *m*, the vibration at mf_c can be suppressed by using CPS-PWM to change the order of the electromagnetic force at mf_c. Therefore, the vibration suppression method is effective for vibration at all multiples of the carrier frequency, not limited to the vibration at $2f_c$.

If the carrier phase angle *X* is set to 0°, 10°, 20°,..., 90°, the phase of the EM force generated by this module around $2f_c$ would be 0°, 20°, 40°,..., 180°.

The carrier frequency is taken as half of the natural frequency of the 0-order modal and the 3-order modal, which can show the effects of CPS-PWM on the vibration more obviously.

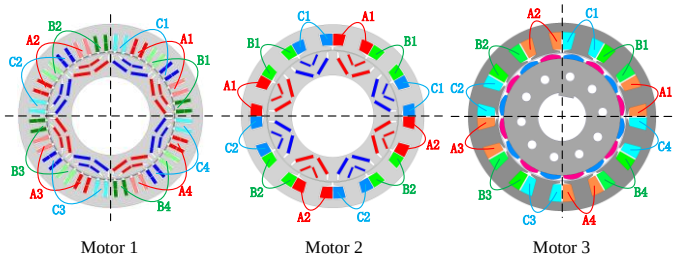

Fig. 10. Structure diagram of motors

TABLE I
PARAMETERS OF MOTORS

Parameter	Motor1	Motor2	Motor3
Slot number	48	12	12
Pole number	8	8	16
Stator OD(mm)	180	180	124
Stator ID(mm)	124	130	85
Air gap(mm)	0.8	0.8	1.4
Rated power(kW)	15.67	15.77	3
Rated speed(rpm)	3000	3000	1000

Fig. 11. Hammer modal test

TABLE II
NATURAL FREQUENCY OF MOTORS

Order	Natural Frequency/Hz		
	Motor 1	Motor 2	Motor 3
2	1990.1	2393.5	2312.2
3	3049.7	3433.9	3262.6
4	4576.8	5427.7	4940.3
0	20127.3	25207.2	18137.4

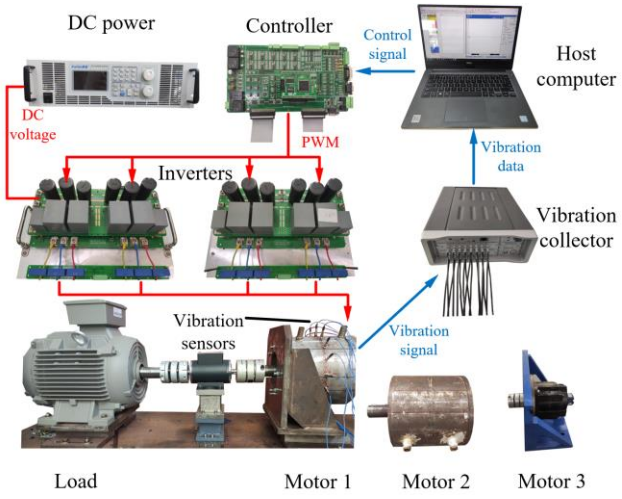

Fig. 12. Experimental platform for motors

B. Experimental results of motor 1

Fig. 13 shows the vibration spectrum under CPC 0-0-0-0 and CPC 0-90-0-90 when the carrier frequency is 10kHz. It can be seen from the spectrum that the vibration amplitude at around $2f_c$ is the largest. Comparing the two spectrums, we can see that in the case of 0-90-0-90, the vibration amplitude at around $2f_c$ is reduced by about 50%.

When f_c =10kHz, there exists $2f_c \approx f_{n0}$, where f_{n0} is the 0-order modal natural frequency. Therefore, there exists the relationship of $|H(0,2\omega_c)| >> |H(3,2\omega_c)| > |H(2,2\omega_c)|$.

When CPC is 0-0-0-0, the theoretical vibration amplitude around $2f_c$ is $|Y_{0\text{-}0\text{-}0\text{-}0}| = f_{m0}|H(0,2\omega_c)| = f_m|H(0,2\omega_c)|$.

When CPC is 0-90-0-90, the theoretical vibration amplitude around $2f_c$ is

$$\begin{aligned}|Y_{0\text{-}90\text{-}0\text{-}90}| &= |f_{m2}H(2,2\omega_c)| + |f_{m6}H(6,2\omega_c)| + |f_{m10}H(10,2\omega_c)| + \dots \\ &\approx f_{m2}|H(2,2\omega_c)| \\ &= 1.25 f_m |H(2,2\omega_c)|\end{aligned}$$

Since $|H(0,2\omega_c)| >> |H(2,2\omega_c)|$, so $|Y_{0\text{-}0\text{-}0\text{-}0}| >> |Y_{0\text{-}90\text{-}0\text{-}90}|$.

Therefore, the vibration amplitude at around $2f_c$ is reduced in the case of 0-90-0-90.

It can be seen from Fig. 13 that the vibration is reduced by about 50%, and the vibration reduction effect is not as good as the theoretical analysis. In the theoretical analysis, the motor stator is regarded as an ring without thickness. But the actual motor has a casing, coils, and it is a slotted design, which prevents the motor stator from an ideal ring and affects the vibration reduction effect.

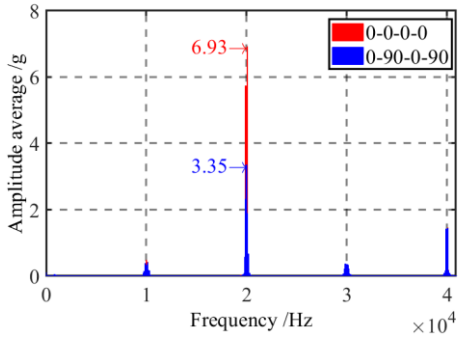

Fig. 13. Vibration spectrum when $f_c = 10\text{kHz} \approx f_{n0}/2$

Fig. 14 shows the vibration amplitudes at around $2f_c$ under different CPCs when the carrier frequency is 10kHz. As the carrier phase angle X increases, the vibration amplitude gradually decreases. In the case of the same X, the vibration amplitude under 0-X-0-X is smaller than that under 0-0-X-X.

The vibration at around $2f_c$ can be expressed as:

$$\begin{aligned}|Y_{0\text{-}X\text{-}0\text{-}X}| &= f_{m0}|H(0,2\omega_c)| + f_{m2}|H(2,2\omega_c)| + f_{m6}|H(6,2\omega_c)| \dots \\ &\approx f_{m0}|H(0,2\omega_c)| + f_{m2}|H(2,2\omega_c)|\end{aligned} \quad (26)$$

$$\begin{aligned}|Y_{0\text{-}0\text{-}X\text{-}X}| &= f_{m0}|H(0,2\omega_c)| + f_{m1}|H(1,2\omega_c)| + f_{m3}|H(3,2\omega_c)| \dots \\ &\approx f_{m0}|H(0,2\omega_c)| + f_{m3}|H(3,2\omega_c)|\end{aligned} \quad (27)$$

As shown in Fig. 8 and Fig. 9, when the CPA X increases, the magnitude of the 0-order EM force f_{m0} gradually decreases, so the first term in Formula (26) and (27) gradually decreases. Therefore, the vibration at $2f_c$ also decreases gradually.

Since $|H(2,2\omega_c)| < |H(3,2\omega_c)|$, the second term in Formula (26) is less than that in Formula (27), so the vibration amplitude under 0-X-0-X is smaller than that under 0-0-X-X.

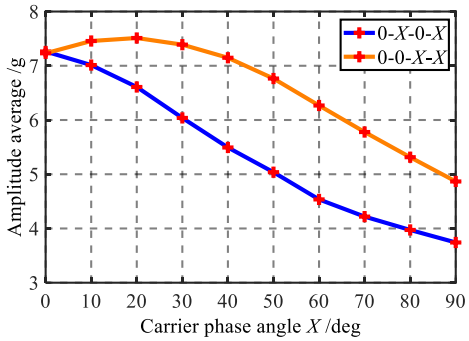

Fig. 14. Vibration Amplitude at around $2f_c$ versus CPA when $f_c = 10\text{kHz} \approx f_{n0}/2$

Fig. 15 shows the vibration spectrums under CPC 0-0-0-0 and CPC 0-0-90-90 when the carrier frequency is 1500Hz. We can see that in the case of 0-0-90-90, the vibration amplitude at around $2f_c$ increased by 30 times.

When f_c =1500Hz, there are: $2f_c \approx f_{n3}$, where f_{n0} is the 0-order modal natural frequency. Therefore, there exists the relationship of $|H(3,2\omega_c)| >> |H(2,2\omega_c)| >> |H(0,2\omega_c)|$.

When CPC is 0-0-0-0, the theoretical vibration amplitude at around $2f_c$ is $|Y_{0\text{-}0\text{-}0\text{-}0}| = f_{m0}|H(0,2\omega_c)| = f_m|H(0,2\omega_c)|$.

When CPC is 0-0-90-90, the theoretical vibration amplitude at around $2f_c$ is

$$\begin{aligned}|Y_{0\text{-}0\text{-}90\text{-}90}| &= |f_{m1}H(1,2\omega_c)| + |f_{m3}H(3,2\omega_c)| + |f_{m5}H(5,2\omega_c)| + \dots \\ &\approx f_{m3}|H(3,2\omega_c)| \\ &= 0.43 f_m |H(3,2\omega_c)|\end{aligned}$$

Since $|H(3,2\omega_c)| >> |H(0,2\omega_c)|$, so $|Y_{0\text{-}0\text{-}90\text{-}90}| >> |Y_{0\text{-}0\text{-}0\text{-}0}|$.

Therefore, the vibration amplitude at around $2f_c$ is greatly increased in the case of 0-0-90-90.

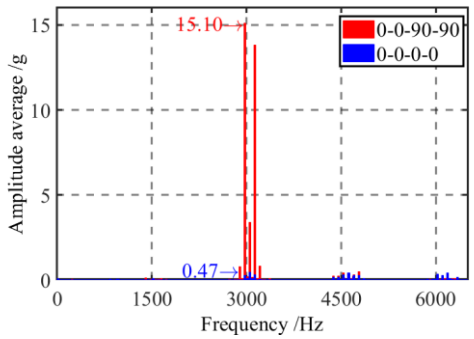

Fig. 15. Vibration spectrum when $f_c = 1500\text{Hz} \approx f_{n3}/2$

Fig. 16 shows the vibration amplitudes at around $2f_c$ under different CPCs when the carrier frequency is 1500Hz. As can be seen from the figure, when the CPA X increases, the vibration amplitude gradually increases. In the case of the same CPA X, the vibration amplitude under 0-X-0-X is smaller than that under 0-0-X-X.

Since $|H(3,2\omega_c)| >> |H(2,2\omega_c)| >> |H(0,2\omega_c)|$, the vibration at around $2f_c$ can be expressed as

$$|Y_{0\text{-}X\text{-}0\text{-}X}| = f_{m0}|H(0,2\omega_c)| + f_{m2}|H(2,2\omega_c)| + f_{m6}|H(6,2\omega_c)|\cdots \approx f_{m2}|H(2,2\omega_c)| \quad (28)$$

$$|Y_{0\text{-}0\text{-}X\text{-}X}| = f_{m0}|H(0,2\omega_c)| + f_{m1}|H(1,2\omega_c)| + f_{m3}|H(3,2\omega_c)|\cdots \approx f_{m3}|H(3,2\omega_c)| \quad (29)$$

As shown in Fig. 8 and Fig. 9, as the CPA X increases, f_{m2} and f_{m3} gradually increase. Therefore, the vibration at $2f_c$ also decreases gradually.

Since $|H(2,2\omega_c)| < |H(3,2\omega_c)|$, the vibration amplitude under 0-X-0-X is smaller than that under 0-0-X-X.

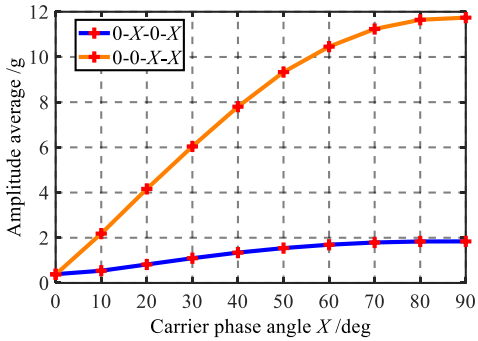

Fig. 16. Vibration Amplitude at around $2f_c$ versus CPA when $f_c = 1500\text{Hz} \approx f_{n3}/2$

C. Experimental results of 12-slot 8-pole motor

The motor is a 2-module motor, so there is only one type of CPC, namely 0-X. It can be seen from the motor structure in Fig. 10 that 0-X in the two-module motor can be equivalent to 0-0-X-X in the four-module motor.

Experiments were carried out when the carrier frequency was 1700 Hz and 12500 Hz. The experimental results are shown in Fig. 17, Fig. 18 and are very similar to the experimental results of motor 1.

The motor used is of fractional slot with concentrated windings, so the spatial order of the EM force is relatively complex, containing not only the 0-order. However, it can be seen from Fig. 17 that the vibration can still be reduced by CPS-PWM, although the vibration suppression effect is not as good as that of integer slot motors.

Similarly, when the carrier frequency of 2 times is close to the natural frequency of the 3-order modal, using the CPS-PWM, the HF vibration is greatly increased.

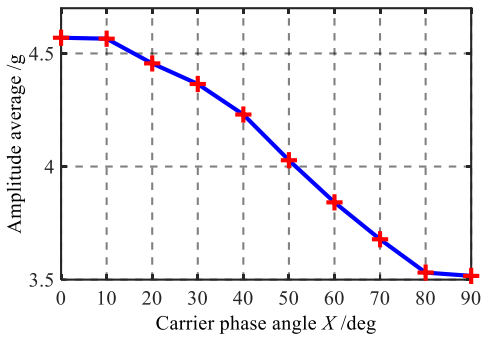

Fig. 17. Vibration Amplitude at around $2f_c$ versus CPA when $f_c = 12.5\text{kHz} \approx f_{n0}/2$

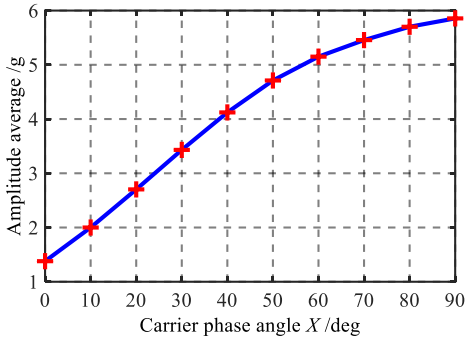

Fig. 18. Vibration Amplitude at around $2f_c$ versus CPA when $f_c = 1700\text{Hz} \approx f_{n3}/2$

D. Experimental results of 12-slot 16-pole motor

Experiments were carried out when the carrier frequency was 1600 Hz and 9000 Hz. The experimental results are shown in Fig. 19, Fig. 20 and are very similar to the experimental results of motor 1.

The motor used is of fractional slot with concentrated windings, and each module contains two pairs of magnetic poles. However, it can be seen from Fig. 19 that the vibration can still be reduced by CPS-PWM.

Through the above three sets of motor experiments, it can be seen that the structure of the PMSM does not affect the vibration suppression effect of CPS-PWM. As long as the motor is a multi-module PMSM, the HF EM vibration can be suppressed by the using the proper CPS-PWM.

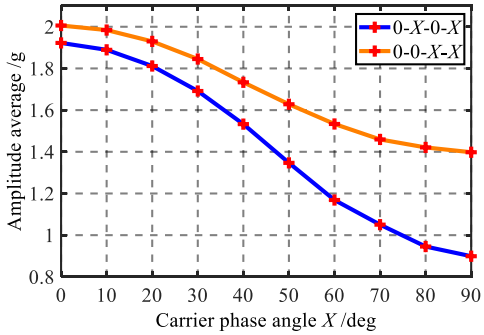

Fig. 19. Vibration Amplitude at around $2f_c$ versus CPA when $f_c = 9000\text{Hz} \approx f_{n0}/2$

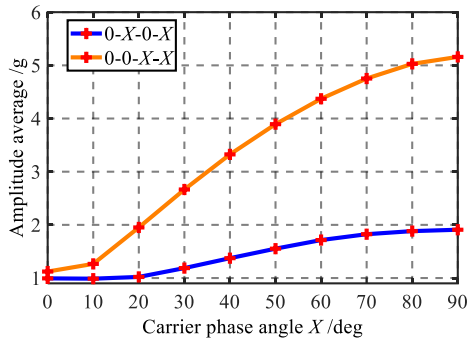

Fig. 20. Vibration Amplitude at around $2f_c$ versus CPA when $f_c = 1600\text{Hz} \approx f_{n3}/2$

VII. Conclusion

This paper proposes a HF PWM EM vibration suppression method, which can suppress vibration by changing the order of the EM force. In this paper, the principle of vibration suppression is theoretically analyzed, and the effectiveness of the method is verified by experiments. The following conclusions can be drawn.

1) At a specific carrier frequency, that is, when the carrier frequency multiplier is close to the 0-order modal natural frequency, the HF vibration of the multi-module motor can be effectively reduced by adopting the proper CPS-PWM. However, when the carrier frequency multiplier is close to the natural frequency of the 2-order or 3-order modal, the HF vibration may increase under CPS-PWM.
2) The 0-order EM force can be transformed to the 2-order or 3-order force by the CPS-PWM of 0-*X*-0-*X* or 0-0-*X*-*X*. The order of the main EM force under 0-*X*-0-*X* is lower, so 0-*X*-0-*X* is better at HF vibration reduction.
3) This vibration suppression method is suitable for multi-module PMSMs and is not affected by the structure of the stator or rotor. But the EM force order distribution of integer slot motor is relatively simple, and therefore the vibration suppression effect of integer slot motor is better.

TABLE III
VIBRATION TEST RESULTS OF MOTORS

Vibration/g		Motor1	Motor2	Motor3
$f_c \approx f_{n0}/2$	SVPWM	7.26	4.57	1.92
	CPS-PWM 0-0-90-90	4.87	3.51	1.40
	CPS-PWM 0-90-0-90	3.74		0.90
$f_c \approx f_{n3}/2$	SVPWM	0.39	1.37	0.99
	CPS-PWM 0-0-90-90	11.74	5.86	5.16
	CPS-PWM 0-90-0-90	1.83		1.91

Acknowledgment

This work is supported by the National Natural Science Foundation of China under Project 52077088.

References

[1] S. Yan, Q. Wang, Y. Xu, Z. Liu, H. Fang and D. Jiang, "Research on High Frequency Vibration Reduction Using Carrier Phase Shifted PWM for 4 3-Phase Windings Permanent Magnet Synchronous Motor," 2021 IEEE Energy Conversion Congress and Exposition (ECCE), Vancouver, BC, Canada, 2021, pp. 4468-4472.
[2] A. Mohammadpour and L. Parsa, "Global Fault-Tolerant Control Technique for Multiphase Permanent-Magnet Machines," in IEEE Transactions on Industry Applications, vol. 51, no. 1, pp. 178-186, Jan.-Feb. 2015.
[3] Z. Liu, L. Fang, D. Jiang and R. Qu, "A Machine-learning Based Fault Diagnosis Method with Adaptive Secondary Sampling for Multiphase Drive Systems," in IEEE Transactions on Power Electronics.
[4] X. Peng, Z. Liu, and D. Jiang, "A review of multiphase energy conversion in wind power generation, " Renewable and Sustainable Energy Reviews, vol. 147, p. 111172, Sep. 2021.
[5] E. Zeze, and K. Akatsu, "Research on vibration analysis and noise-reduction technique of PM motor," in 2012 XXth InternationalConference on Electrical Machines, Marseille, 2012, pp. 458-463.
[6] Zhi Yang, S. Yaman and M. Krishnamurthy, "Mitigation ofEM vibration in PMSM:A rotor positio n related variablecarrier frequency technique," in 2017 IEEE TransportationElectrification Conference and Expo (ITEC), Chicago, IL, 2017, pp.448-452.
[7] I. P. Tsoumas, and H. Tischmacher, "Influence of the inverter'smodulation technique on the audible noise of electric motors," in 2012XXth International Conference on Electrical Machines, Marseille,2012, pp. 2981-2987.
[8] F. Yuan, S. Huang, and Q. Hao, "Research on High FrequencyVibration Suppression of Permanent Magnet Motor Using CarrierPhase Shift Technology," in Electric Machines and Control,2014,(7):12-17.
[9] W. Zhang, Y. Xu, H. Huang and J. Zou, "Vibration Reduction for Dual-Branch Three-Phase Permanent Magnet Synchronous Motor WithCarrier Phase-Shift Technique," in IEEE Transactions on PowerElectronics, vol. 35, no. 1, pp. 607-618, Jan. 2020.
[10]X. Li, C. Liu, and B. Mei, "Analysis of Vibration and Noise Source ofElectric Vehicle IPMSM Wide Range Speed Regulation," in ElectricMachines and Control,2018,38(17):5219-5227+5319.
[11]C. Liao, W. Jiang and Z. Zhang, "Analysis of EMVibration Characteristics of An Interior Permanent MagnetSynchronous Motor," in 2019 22nd International Conference onElectrical Machines and Systems (ICEMS), Harbin, China, 2019, pp.1-5.
[12]S. Wang, J. Hong, Y. Sun and H. Cao, "Analysis of Zeroth-Mode Slot Frequency Vibration of Integer Slot Permanent-Magnet Synchronous Motors," in IEEE Transactions on Industrial Electronics, vol. 67, no. 4, pp. 2954-2964, April 2020.
[13]Y. -S. Lai, W. -T. Lee, Y. -K. Lin and J. -F. Tsai, "Integrated Inverter/Converter Circuit and Control Technique of Motor Drives With Dual-Mode Control for EV/HEV Applications," in IEEE Transactions on Power Electronics, vol. 29, no. 3, pp. 1358-1365, March 2014.
[14]G. Vidmar and D. Miljavec, "A Universal High-Frequency Three-Phase Electric-Motor Model Suitable for the Delta- and Star-Winding Connections," in IEEE Transactions on Power Electronics, vol. 30, no. 8, pp. 4365-4376, Aug. 2015.
[15] Pulse Width Modulation for Power Converters Principles and Practice[M]. John Wiley & Sons Inc, 2003.

Zicheng Liu (M'18) was born in Shandong, China, in 1989. He received the B.S. degree in Hydropower Engineering from Huazhong University of Science and Technology (HUST), Wuhan, China, in 2011, and the Ph.D. degree in Electrical Engineering from Tsinghua University, Beijing, China, in 2016. During Otc. 2014 to Mar. 2015, he was a Visiting Student at Purdue University, West Lafayette, IN, USA. During Jun. 2016 to Sep. 2018, he was a postdoc researcher at Beijing Jiaotong University, Beijing, China. He is currently an associate professor at HUST. His research interests include multiphase motor control systems and transportation electrification.

She Yan was born in Jiangxi, China, in 1999. He received the B.S. degree in Electrical Engineering from the Huazhong University of Science and Technology, Wuhan, China, in 2021, where he is currently working toward the M.S. degree in Electrical Engineering with the School of Electronic and Electrical Engineering. His main research interests are motor control and motor vibration.

Haiyang Fang (Member, IEEE) was born in Hubei, China. He received the B.M.E. degree in mechanical engineering and the Ph.D. degree in electrical engineering from the Huazhong University of Science and Technology, Wuhan, China, in 2013 and 2018, respectively. His research interests include mechanical design and vibro-acoustic analysis of electrical machines.

Dong Jiang (S05'-M12'-SM16') received B.S and M.S degrees in electrical engineering from Tsinghua University, Beijing, China, in 2005 and 2007 respectively. He began his Ph.D. study in Center for Power Electronics Systems (CPES) in Virginia Tech in 2007 and was transferred to University of Tennessee with his advisor in 2010. He received his Ph.D. degree in power electronics and motor drives from University of Tennessee in Dec. 2011. He was with United Technologies Research Center (UTRC) in Connecticut as a Senior Research Scientist/Engineer from Jan 2012 to July 2015. He has been with Huazhong University of Science &Technology (HUST) in China as a professor since July 2015. Dong Jiang's major research area is power electronics and motor drives, with more than 40 published IEEE journal and conference papers in this area. He has two best paper awards in IEEE conferences. He is an associate editor of IEEE Transactions on Industry Applications.

Ronghai Qu (Fellow, IEEE) was born in China. He received the B.E.E. and M.S.E.E. degrees in electrical engineering from Tsinghua University, Beijing, China, in 1993 and 1996, respectively, and the Ph.D. degree in electrical engineering from the University ofWisconsin-Madison, Madison, WI, USA, in 2002. In 1998, he joined theWisconsin Electric Machines and Power Electronics Consortiums as Research Assistant. He became a Senior Electrical Engineer with Northland, a Scott Fetzer Company in 2002. Since 2003, he had been with the General Electric (GE) Global Research Center, Niskayuna, NY, USA, as a Senior Electrical Engineer with the Electrical Machines and Drives Laboratory. He has authored more than 120 published technical papers and is the holder of more than 50 patents/patent applications. From 2010, he has been a Professor with the Huazhong University of Science &Technology, Wuhan, China. Prof. Qu is a full member of Sigma Xi. He has been the recipient of several awards from GE Global Research Center since 2003, including the Technical Achievement and Management Awards. He is also the recipient of the 2003 and 2005 Best Paper Awards, and third prize from the Electric Machines Committee of the IEEE Industry Applications Society at the 2002 and 2004 IAS Annual Meeting.

Dear Editors and Reviewers,

Thanks so much for the valuable comments and advices on our manuscript entitled *Research on High Frequency Vibration Reduction Using Carrier Phase Shifted PWM for 4-module 3-phase Permanent Magnet Synchronous Motor*. We have studied the comments carefully and have made important changes to the manuscript. Revised portions are marked in red or highlighted in the paper. The modifications in the paper and the responses to the reviewer's comments are as following:

List of Changes:

1. We rewrote the whole manuscript to correct grammar mistakes and reduce redundant sentences.
2. We mentioned the cost increase of the motor drive system used in the paper in the section II, which makes the paper more objective.
3. We revised the topology diagram of the motor drive system (Fig. 2) to make it easier to understand.
4. We added more analysis details in Section IV B to make the vibration reduction principle clearer.
5. We combined the structure diagrams of the three motors into one diagram(Fig. 10) to make the paper more concise.
6. We introduced the details of modal test in Section VI part A.
7. We combined the modal natural frequency tables of the three motors into one table(Table II) to make the paper more concise.
8. We revised the diagram of the motor vibration experiment platform (Fig. 12) to make it easier to understand.
9. We added a summary table(Table III) of vibration experiments to better show the experimental results.

Response to the Associate Editor:

1. Dear authors, this manuscript submission was carefully reviewed. According to the reviewers' comments, the present form of this manuscript needs further revisions. Please carefully revise the paper, completely address all the comments from the reviewers, and resubmit the manuscript, before a decision can be made.

Thanks for your important suggestion. We gave point-to-point responses to all the reviewers' questions in the reply letter. And we also made important revisions to the manuscript.

First of all, we added more detailed description of the motor system used in the paper. Secondly, we added analysis details in Section IV B to make the vibration reduction principle easier to understand. Then, we added the details and diagrams(Fig. 11 and Fig. 12) of the motor modal test and vibration experiments in the revised manuscript, and described the experiments in detail in the reply letter (in Q5 and Q6 of Reviewer 2). Finally, we simplified the sentences and modified the structure of the

paper to make it more readable.

Response to Reviewer 1:

1. When the carrier phase-shifted angle is 0, the vibration performances under 0-*X*-0-*X* and 0-0-*X*-*X* modes should be the same. But why are they different in Figure 20?

Thanks for your question. In theory, when the carrier phase *X* is 0, both 0-*X*-0-*X* and 0-0-*X*-*X* can be equivalent to 0-0-0-0. Therefore, the amplitude of vibration should be exactly the same in the two conditions. However, the vibration amplitudes in Fig. 20 (now Fig 19 in revision) are different. Similarly in Fig. 21 (now Fig 20 in revision), when the carrier phase *X* is 0, the vibration of the motor at 0-*X*-0-*X* and 0-0-*X*-*X* is not exactly the same, either. Errors may arise from experimental errors and measurement errors.

For experimental errors, the experiments under the two conditions are carried out successively. During the experiment, the motor will heat up and change the parameters of the motor, so the vibrations emitted by the motor are not exactly the same when the two groups of experiments are conducted. This phenomenon is more obvious for low power-rating motors, like Motor 3 in the paper, which corresponds to Figs. 19 and 20 in the revision. However, for high power-rating motors at no-load test, the variation of parameters due to heat is much weaker. Therefore, the vibration under 0-*X*-0-*X* and 0-0-*X*-*X* for Motors 1 are almost the same, which correspond to Figs. 14 and 16 in the revised manuscript.

Moreover, unavoidable measurement errors exist during the vibration experiments. When measuring vibration, the vibration acquisition instrument will select a suitable length of vibration data for spectrum analysis. The actual vibration of the motor is not completely periodic, and there will be some fluctuations. Therefore, different vibration time series data may be selected each time the vibration is measured, resulting in different vibration results.

2. How is the motor vibration performance, when the carrier phases of the four groups are all different? Would it be better or worse? Could you please give some comments or explanations?

Thanks for your question. From the Section IV of the paper, we can draw the following conclusions:

(1) The electromagnetic force can only act with the same order modal or the same order transfer function to excite vibration.

(2) For the integer slot motor we studied, the high-frequency EM force in the motor is dominated by 0-order.

(3) When the electromagnetic force order is close to the natural frequency of a certain order modal, the effect of this order modal is much greater than that of other orders.

Without Carrier phase-shifted, the electromagnetic force in the motor is the 0-order electromagnetic force, which only interacts with the 0-order modal or the 0-

order transfer function to generate vibration, and the vibration is Y_0 in Fig. R1(a).

Using CPS-PWM with carriers phase 0-90-0-90 or 0-0-90-90, the electromagnetic force can almost be changed to other-order electromagnetic force, such as 2-order electromagnetic force. Then the 2-order electromagnetic force only interacts with the 2-order modal or the 2-order transfer function to generate vibration, and the vibration is Y_2 in Fig. R1(b).

The effect of the 0-order modal near the natural frequency of the 0-order modal is much greater than that of the 2-order modal, so $Y_0 >> Y_2$. By using CPS-PWM, the vibration is greatly reduced.

Of course, the 0-order electromagnetic force can hardly be completely transformed into other-order electromagnetic force under CPS-PWM. When the 0-order electromagnetic force is partially transformed into other order electromagnetic forces, the vibration is jointly generated by the 0-order electromagnetic force and other order electromagnetic forces. However, because the effect of the 0-order modal near the natural frequency of the 0-order modal is much greater than that of the 2-order modal, the proportion of the vibration generated by the 0-order electromagnetic force is much larger than that generated by other orders. Therefore, in this condition, the vibration mainly depends on the proportion of the 0-order electromagnetic force.

When all the four carriers are different, denoted as 0-*X*-*Y*-*Z*, which can be regarded as the combination of 0-X_1-0-X_1 and 0-0-X_2-X_2. In this case, the proportion of the 0-order electromagnetic force needs to be analyzed in combination with the specific carriers phase *X*,*Y* and *Z*. Here we can take one of the special cases for analysis. For example, for 0-*0*-*Y*-*Z*, the content change of the 0-order electromagnetic force is shown in Fig. R2. It can be seen from Fig. R2 that the 0-order electromagnetic force proportion is higher than that of 0-0-*X*-*X*, so its vibration suppression effect is worse than that of 0-0-*X*-*X*.

For 0-*X*-*Y*-*Z*, the vibration needs to be analyzed in combination with the specific carriers phase *X*,*Y* and *Z*. But it is certain that the vibration suppression effect under 0-*X*-*Y*-*Z* is not as good as 0-90-0-90 and 0-0-90-90, because in the latter two cases, the proportion of 0-order electromagnetic force is 0.

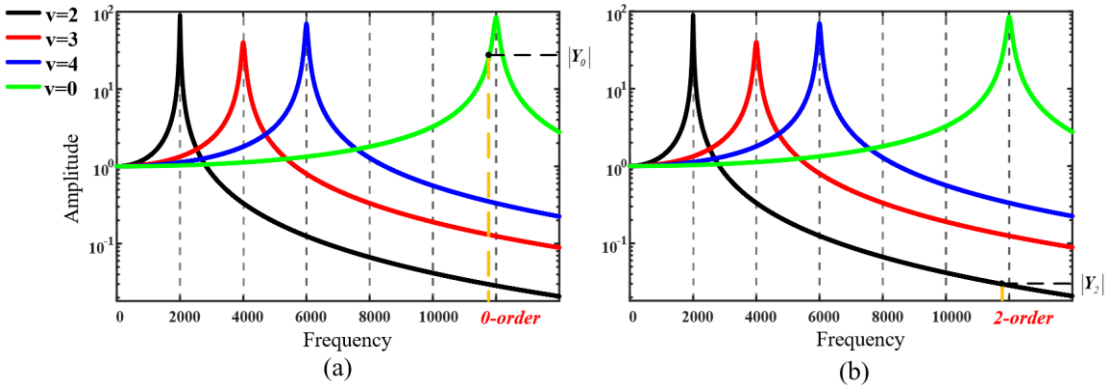

Fig. R1 Motor mechanical transfer function

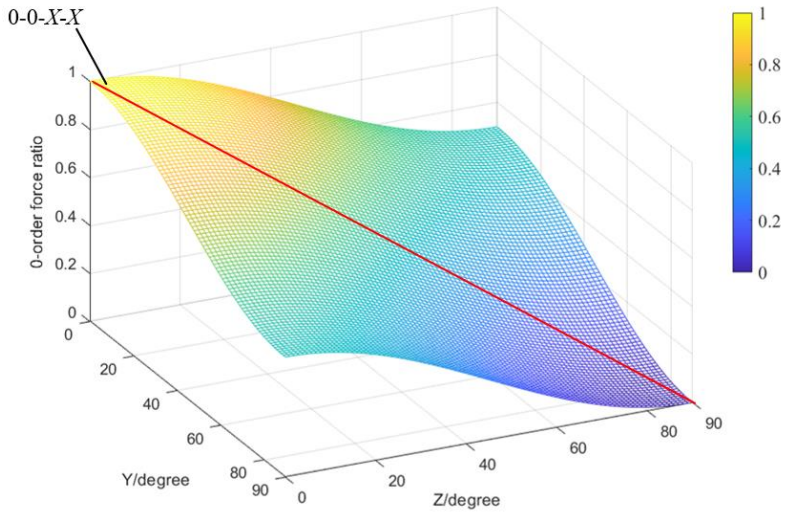

Fig. R2 Proportion change of 0-order electromagnetic force under 0-0-*Y*-*Z*

3. When the carrier frequency is close to the 0-order mode natural frequency, the vibration can be reduced by using CPS-PWM. Similarly, when the carrier frequency is closed to the 2nd or 3rd mode natural frequency, can the vibration be reduced by changing the EM force order through CPS-PWM?

Thanks for your question.

Without Carrier phase-shifted, the electromagnetic force in the motor is the 0-order electromagnetic force, which only interacts with the 0-order modal or the 0-order transfer function to generate vibration. Using CPS-PWM, the 0-order electromagnetic force can be changed to other order electromagnetic force, such as 2-order electromagnetic force. Then the 2-order electromagnetic force only interacts with the 2-order modal or the 2-order transfer function to generate vibration.

When the carrier frequency is close to the 0-order modal natural frequency, the effect of the 0-order modal is much greater than that of the other order modal, as shown in Fig. R1. Therefore, the vibration generated by the 0-order electromagnetic force without carrier phase-shifted is much larger than the vibration generated by other orders electromagnetic force under CPS-PWM. Using CPS-PWM, the vibration is suppressed.

When the carrier frequency is close to the 2-order modal natural frequency, the effect of electromagnetic force of 0-order is much smaller than that of other order, especially 2-order, as shown in Fig. R1. Therefore, the vibration without carrier phase-shifted generated by the 0-order electromagnetic force is much small than the vibration generated by other orders electromagnetic force under CPS-PWM. Using CPS-PWM, the vibration is greatly reduced.

Therefore, when the carrier frequency is close to the 2nd (or 3rd) modal natural frequency, the vibration would be worse by using CPS-PWM.

4. In addition to the vibration at 2 times the carrier frequency, can the vibration at other multiples of the carrier frequency also be reduced by CPS-PWM?

Thanks for your question. we added more details about this point in section VI of the revised manuscript. When the carrier phase changes by X, the phase of the electromagnetic force at m times the carrier frequency changes by mX. Therefore, for the electromagnetic force of all multiples the carrier frequency, the phase of the electromagnetic force can be changed by changing the carriers phase, thereby changing the order of the electromagnetic force and achieving the vibration suppression. For the vibration at different multiples the carrier frequency, in order to achieve the same vibration suppression effect, the required carriers phase may be different. For example, in order to achieve the best vibration reduction effect, for the vibration at twice the carrier frequency, the required carriers phase is 0-90-0-90 and for the vibration at the carrier frequency, the required carriers phase is 0-180-0-180. Generally speaking, the vibration amplitude at 2 times the carrier frequency is highest, so the paper mainly analyzes the vibration at 2 times the carrier frequency. But the CPS-PWM has a suppression effect on the vibration at multiples the carrier frequency.

Response to Reviewer 2:

1. Four sets of the inverter will require four more number of switches and microcontrollers. Can the authors justify the increasing cost of the proposed system?

Thanks for your question. Compared with the traditional motor system, the parallel inverter powered multi-module motor system proposed in the paper does require more hardware cost, which has been mentioned in the revised manuscript. One traditional three-phase inverter is substituted by four three-phase inverters, with each of them being 1/4 power rating of the traditional three-phase one.

The control chip adopted is TMS320F28377D, which has 12 sets of PWM output pins, which are enough for 4 inverters. The four inverters are controlled by the one controller,so the cost of the controller will not increase.

The hardware system of parallel inverters and multi-module motor used in the paper can not only be used for high-frequency vibration suppression, but also be used to achieve common-mode voltage suppression, reduce common-mode EMI[R1], and have better fault tolerance[R2]. Although the cost of switching devices increases, it does help to improve the fault tolerance of the motor system, reduce common-mode EMI and high-frequency vibration.

2. Control of four sets of three-phase require ways to communicate with each other to adjust phase. Can authors put more details on How does the controller and inverter talk to each other?

Thanks for your reminding. The control block diagram of the motor system is shown in Fig. R3. It should be noted here that all four inverters are controlled by the one controller, so there is no communication problem between the controllers. We updated Fig. 2 in the revision, which shows that one controller is adopted to adjust all the four three-phase inverters.

As shown in Fig. R3, the speed signal and current signals of four inverters

collected by the sensors are sent to the same controller. The controller calculates the duty cycles of the four PWM groups according to the collected signals, and adjusts the phases of the four carriers. Then, PWM pluses are sent by the same controller to the four inverters to drive the 4-module motor.

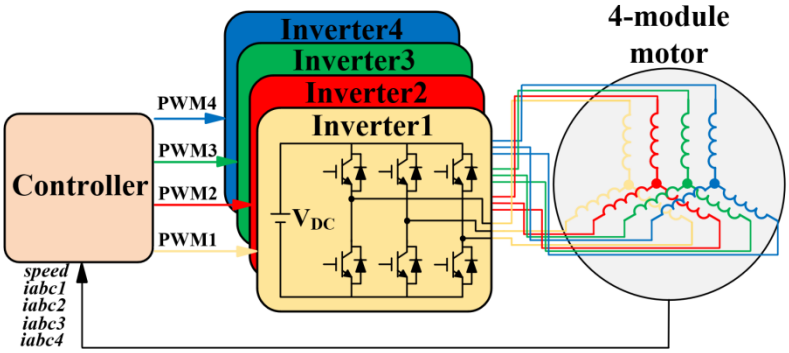

Fig. R3 Schematic of 4-module PMSM drive system

3. Analysis is performed based on the assumption of the perfect balance of the rotor and stator. In practice, perfect balance is very difficult to be manufactured. Will this method be valid with unbalanced machines, which is unavoidable in the real machine?

The three motors used in this experiment are all unbalanced machines, that is we didn't do perfect balance corrections on any of them . From the experimental results, it can be seen that the method proposed in the paper has obvious vibration reduction effect on the all three motors, so it can be proved that the vibration reduction method in the paper is effective for unbalanced motors.

In addition, it can also be proved theoretically that the vibration reduction method is effective for unbalanced motors. The unbalance of the motor will cause the air gap magnetic density to be uneven, resulting in uneven high-frequency electromagnetic force, thereby affecting the high-frequency PWM electromagnetic vibration. In the perfect-balanced motor, the magnitude of the electromagnetic force generated by each module of the multi-module motor should be the same and the force is 0-order, as shown in Fig. R4. In the unbalanced motor, the magnitude of the electromagnetic force generated by each module of the multi-module motor is different and it can be divided to two parts, one part is the 0-order electromagnetic force, which accounts for the main component, and the other is the electromagnetic force caused by the unbalance. The degree of unbalance of the normally-manufactured motor is generally small, so the proportion of the force caused by unbalance is very small. The main vibration generated by the 0-order electromagnetic force can be reduced by the CPS-PWM proposed in the paper, so the vibration of the unbalanced motor will still be reduced obviously.

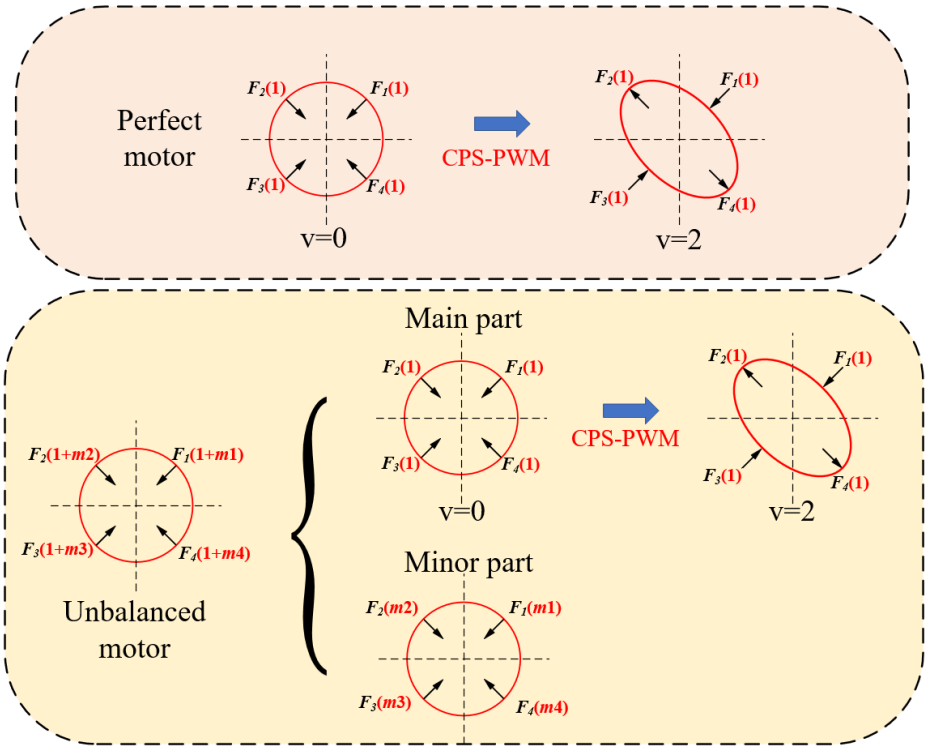

Fig. R4. Order variation of EM force for perfect motor and unbalanced motor

4. If the carrier frequency of PWM is high enough, i.e., f_sw>10kHz, vibration (noise) due to PWM force is very small. More dominant vibration results from force unbalance results from rotor mechanical unbalance during rotations. Can the author put more comments and comparisons of machine noise in general?

Thanks for your question. The vibration of the motor can be roughly divided into two parts: the low frequency part and the high frequency part, as shown in Fig. R5. The low frequency part is mainly caused by eccentricity, low frequency current harmonics and other mechanical factors.The high frequency part is generated by the high frequency PWM current harmonics. Low-frequency vibration and high-frequency vibration have different sources, different frequency ranges, and the two parts do not interfere with each other. In practical engineering, the two parts are also considered separately, that is, one index is set for the low frequency band vibration and another index is set for the high frequency band vibration.

The vibration suppression method in the paper is only aimed at the high-frequency electromagnetic vibration caused by the high-frequency PWM current, and will not affect the low-frequency vibration.

In addition, when the carrier frequency is high enough, the noise of the motor is too high to be recognized by the human ear. However, the high-frequency vibration of the motor still exists. Fig. R5 shows the vibration spectrum of the motor (Motor1 in the paper) when the carrier frequency is 10kHz. It can be seen from the figure that even if the carrier frequency is high enough, the high-frequency electromagnetic vibration still exists and can't be neglected compared to the low-frequency vibration.

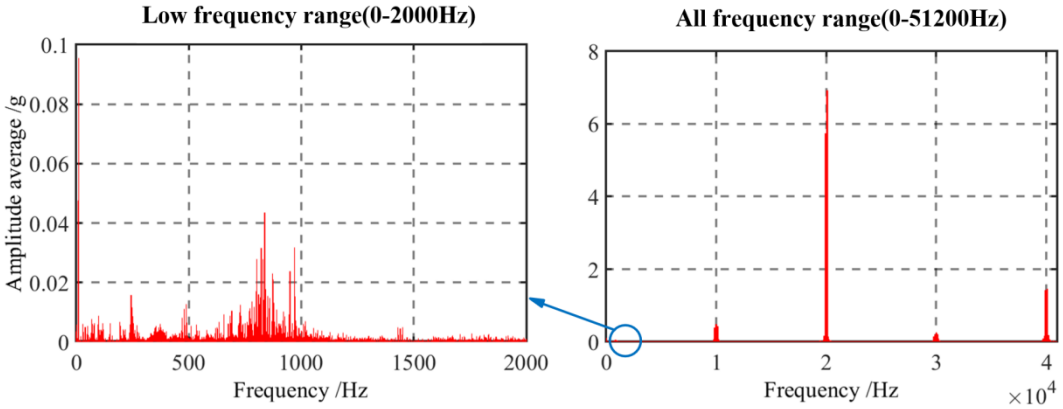

Fig. R5. Motor1 vibration spectrum

5. The noise frequency results from rotation is proportional to the rotating velocity, and the reviewer thinks it will affect the PWM resulting noise. Are the experimental results done when the machine is in a locked position or in a rotation? Can authors put more details on experimental conditions?

Thanks for your question. We are sorry that the experimental process isn't clearly described in the original manuscript, we have added the experimental details in the revised manuscript. During the vibration experiment, the motor was controlled at a constant speed of 600rpm.

Here we analyze the generation mechanism of the PWM vibration. The switching action of the inverter introduces high-frequency current harmonics to motor windings. The high-frequency current harmonics generate a high-frequency magnetic field in the air gap. The high-frequency magnetic field interacts with the fundamental frequency magnetic field to generate a high-frequency electromagnetic force. The high-frequency electromagnetic force acts on the stator and rotor to generate high-frequency PWM electromagnetic vibration and noise. So the high-frequency electromagnetic vibration is essentially generated by the high-frequency harmonic currents and is almost independent from the vibration caused by rotation. Therefore, the vibration generated by the rotation will not affect the PWM vibration and noise.

In addition, the vibration noise generated by rotation and the vibration generated by PWM are located in two different frequency ranges, as shown in Fig. R5, and these two can hardly affect each other.

6. The modal analysis (natural frequencies) performed in the experimental section require more detail. I assume the modal analysis will differ with machine test jig, coupling, and load since they are also mass spring dampers. Will the method still be effective with the machine under load conditions?

Thanks for your question. We are sorry that the process of modal test isn't clearly demonstrated in the original manuscript, we have added the relevant content of modal test in the revised manuscript.

During the modal test,the motor was hoisted by the elastic rope, as shown in Fig. R6. We arrange the vibration acceleration sensors on the motor casing, and hit the motor casing with a force hammer. The force hammer measured the excitation force

signal, and the sensors measured the vibration signal. The signals are received by the vibration collector and sent to the host computer for analysis. By analyzing the excitation force signal and the vibration signal, the mechanical transfer function and the modal natural frequencies can be obtained.

During motor vibration experiment, the motor was installed on the platform, as shown in Fig. R7. When the motor is installed on the platform, the motor mechanical structure is changed and the modal natural frequencies would be different from the natural frequencies measured by the modal test.

However, generally speaking, the radial modals depend on the radial deformation of the effective part of the motor and are less affected by fixation of the platform. To verify the above statement, we tested on a motor. As shown in Fig. R8, the modal test experiments were carried out on the motor in suspended and fixed states, respectively. The measured 2-order modal natural frequencies under these two conditions are 2010.3Hz and 2173.8Hz, with a change rate of 8.1%. The 3-order modal natural frequencies are 3342.0Hz and 3428.5Hz, with a change rate of 2.6%. It can be seen from the results that the modal test error caused by the motor platform(including test jig,coupling and load) is very small and hardly affects the vibration experiment results.

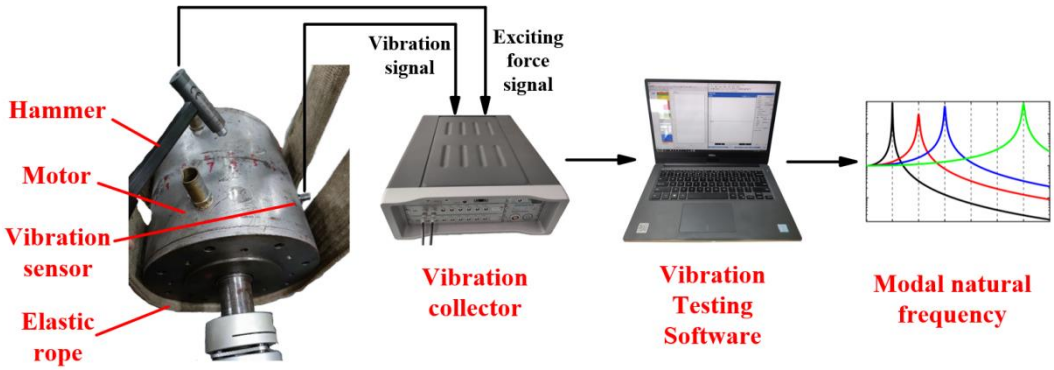

Fig. R6. Motor modal test

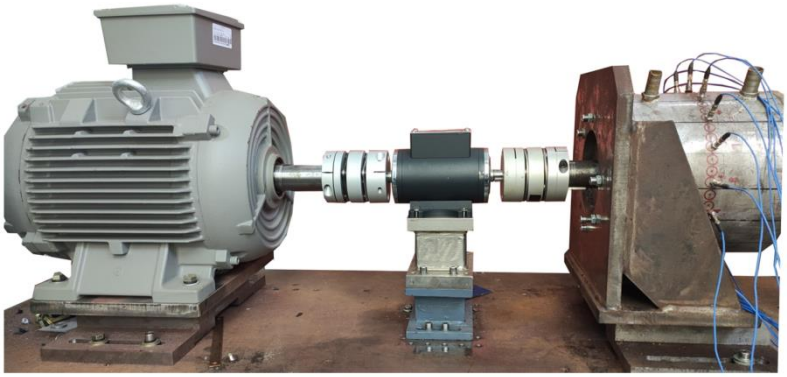

Fig. R7. Motor vibration experiment platform

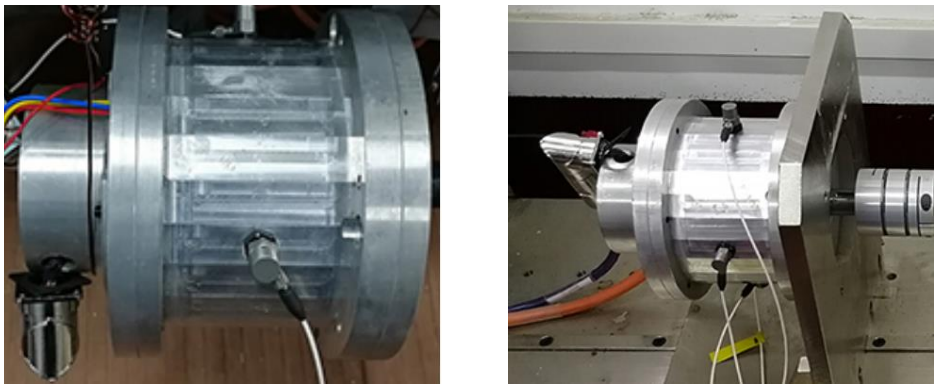

Fig. R8. Motor modal test in suspended and fixed states

7. In figure 13, can the author put more details on how the vibration is measured? The reviewer thinks it would be nicer if the vibration transducer placement and the measurement method were shown in more detail?

Thanks for your question. We are sorry that the process of vibration measurement is not clearly described in the original manuscript. We supplemented the details of vibration measurement in the revised manuscript.

The experimental platform is shown in Fig. R9. The motor was installed on the platform during the experiment. The motor was powered by 4 voltage source inverters. The inverters was controlled by the controller, and the controller communicated with the host computer. During the experiment, the host computer communicated with the controller and sent the control signals to the inverters to drive the motor.

As shown in Fig. R10, 16 vibration acceleration sensors were arranged at equal intervals on the motor casing. The vibration signals collected by the sensors was processed by the vibration acquisition instrument and sent to the host computer for spectrum analysis. The average value of the vibration spectrum of the sensors was calculated to evaluate the motor vibration.

During the experiment, the motor speed was controlled to be 600 rpm, and the vibration data of the motor was collected. Then we changed the carriers phase and repeated the experiment. The change of the high-frequency vibration of the motor under different carriers phase was compared and analyzed.

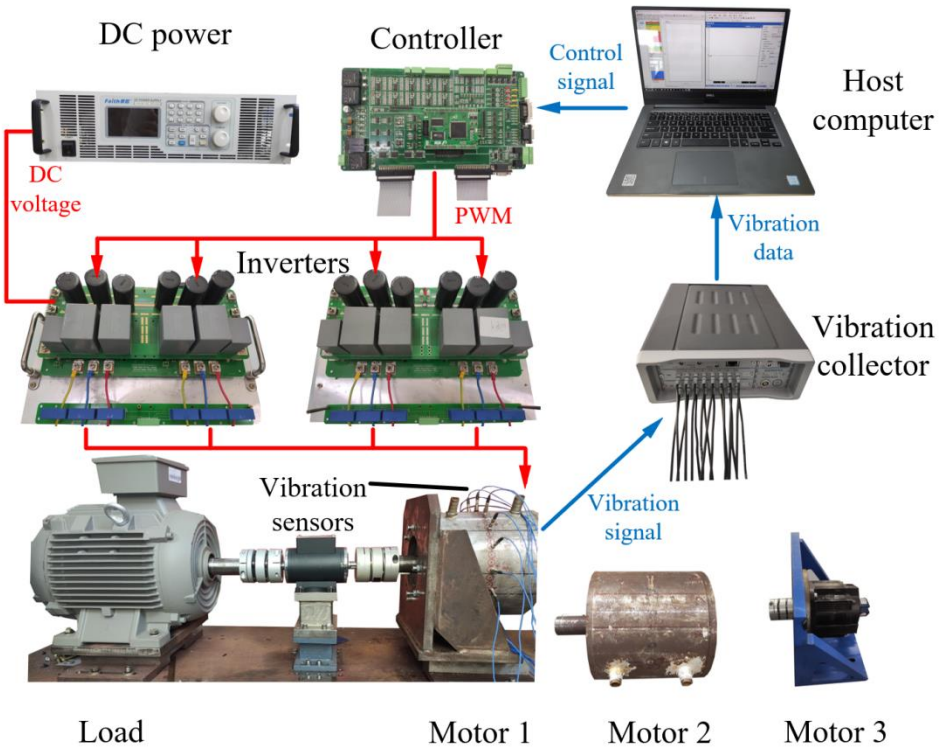

Fig. R9. Motor experiment platform

Fig. R10. Vibration sensors arrangement

8. Looking at figure 7, the force on v=0 is canceled just as same as in the case of v=2. Can authors put a more physically intuitive explanation on force cancellation and noise reduction mechanism? The force cancellation in the most combination in slot/pole of the rotating machine is known. How does the cancellation coupling of two sets of two three-phases better than conventional force cancelation?

Thanks for your question. We are sorry that the principle of vibration reduction is

not well addressed in original manuscript. We added relevant content in the revised manuscript to make the vibration reduction principle more intuitive and easier to understand.

From the paper, we can draw the following conclusions:

(1) The electromagnetic force can only act with the same order modal or the same order transfer function to excite vibration.

(2) For the integer slot motor we studied, the high-frequency EM force in the motor is dominated by 0-order.

(3) When the electromagnetic force order is close to the natural frequency of a certain order modal, the effect of this order modal is much greater than that of other orders.

Without Carrier phase-shifted, the electromagnetic force in the motor is the 0-order electromagnetic force, which only interacts with the 0-order modal or the 0-order transfer function to generate vibration, and the vibration is Y_0 in Fig. R11(a).

Using CPS-PWM, the electromagnetic force can be completely changed to other order electromagnetic force, such as 2-order electromagnetic force, as shown in Fig. R12. Then the 2-order electromagnetic force only interacts with the 2-order modal or the 2-order transfer function to generate vibration, and the vibration is Y_2 in Fig. R11(b).

When the frequency of high-frequency electromagnetic force is close to the natural frequency of the 0-order modal, the effect of the 0-order modal is much greater than that of the 2-order modal, so $Y_0 >> Y_2$. That is, by using CPS-PWM, the vibration is greatly reduced.

The traditional force elimination, as shown in Fig. R13, places two three-phase windings of the dual three-phase motor in the same slot. By setting the two carriers to have a phase difference of 90 °, the magnetomotive forces generated by the two three-phase windings cancel each other out, and the electromagnetic force of twice carrier frequency is eliminated, and thereby realizing vibration suppression[R3]. However, the coupling between the two three-phase windings is very large. Under carrier phase-shifted, the amplitude of the high-frequency harmonic current is greatly increased, and the motor current is seriously distorted, which affects the current loop control performance of the motor. In addition, since the two three-phase windings are located in the same slot, when one three-phase winding fails, the fault can easily spread to the other winding, resulting in poor fault tolerance.

In the multi-module motor used in the paper, the coupling between the three-phase windings is very small, hence the current distortion is very small under carrier phase-shifted. As shown in Fig. R14, the three-phase windings of the motor are located in different areas of the stator, resulting in physical isolation, thermal isolation and electrical isolation, which minimizes the fault propagation between three-phase windings [R4], and has good fault tolerance capability.

The method provided in the paper does not eliminate the electromagnetic force, but changes the spatial form of the electromagnetic force. The magnitude of the electromagnetic force is similar to the original, but the spatial form of the force has changed. So the vibration suppression method proposed in the paper is completely

different from the conventional force cancelation, and we think it is innovative.

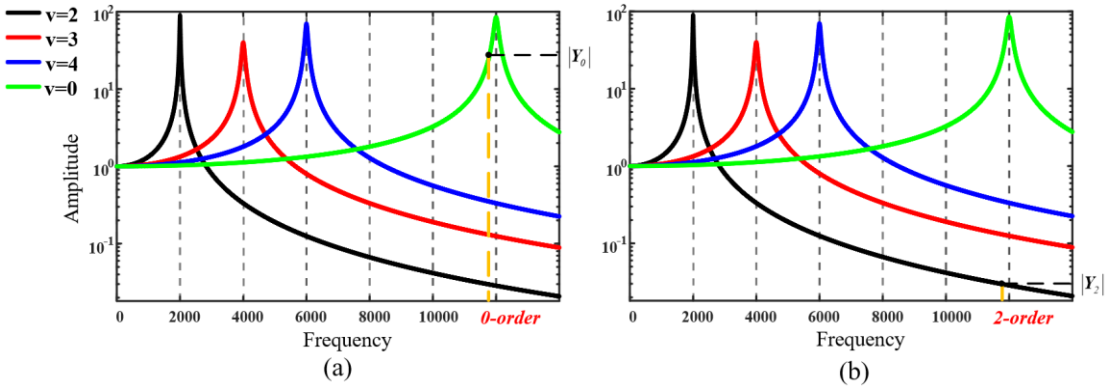

Fig. R11. Motor mechanical transfer function

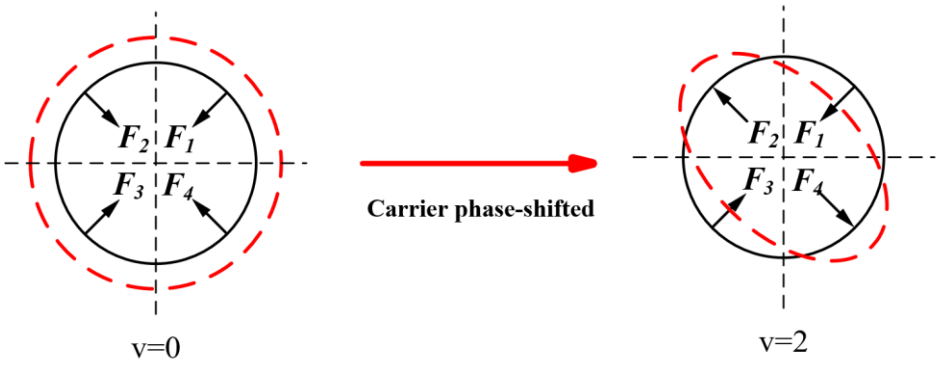

Fig. R12. Schematic diagram of the order change of the EM force

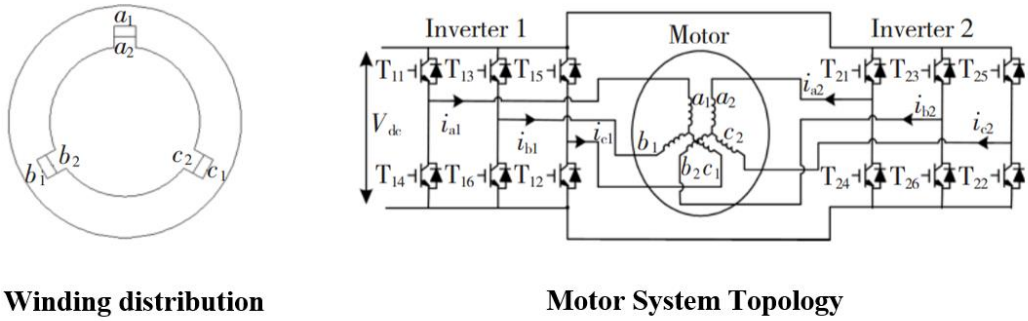

Fig. R13. Winding distribution and topology of dual three-phase motor

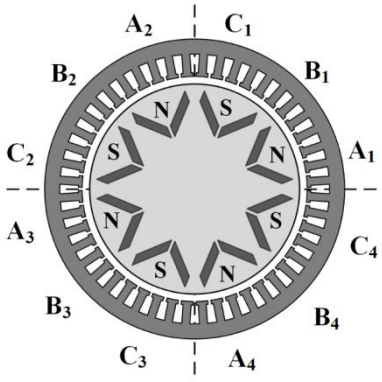

Fig. R14. Structure of the 4-module 3-phase PMSM

References:

[R1] D. Jiang, K. Liu, Z. Liu, Q. Wang, Z. He and R. Qu, "Four-Module Three-Phase PMSM Drive for Suppressing Vibration and Common-Mode Current," in IEEE Transactions on Industry Applications, vol. 57, no. 5, pp. 4874-4883, Sept.-Oct. 2021.doi: 10.1109/TIA.2021.3085542.

[R2] X. Sun, Z. Liu, A. Li, Z. Wang, D. Jiang and R. Qu, "Self-Adaptive Fault-Tolerant Control of Three-Phase Series-End Winding Motor Drive," in IEEE Transactions on Power Electronics, vol. 37, no. 9, pp. 10939-10950, Sept. 2022.doi: 10.1109/TPEL.2022.3160747.

[R3] F. Yuan, S. Huang, Q. He, Vibration reduction control using carrier phase shifted for permanent magnet synchronous motor fed by dual PWM inverters[J]. Electric Machines and Control, 2014,18(07):12-17.DOI:10.15938/j.emc.2014.07.004.

[R4] B. Wang, J. Wang, A. Griffo and Y. Shi, "Investigation Into Fault-Tolerant Capability of a Triple Redundant PMA SynRM Drive," in IEEE Transactions on Power Electronics, vol. 34, no. 2, pp. 1611-1621, Feb. 2019.

Response to Reviewer 3:

1. The paper is written very complexly and is not easy to follow. I believe the paper could have been written much more clearly, with much more detail in the derivation and analysis of the mathematical model and focused on just one machine?

Thanks for your important suggestion. Sorry for not explaining the paper clearly. We added relevant content in revised manuscript to make the paper easier to understand. First, we have added annotations in Fig. 4 to make it more intuitive. And we added analysis details in Section IV B to make the vibration reduction principle easier to understand. Then ,we gave more details on the motor vibration experiments. Last, we added a table(Table III) to summarize the experiment results.

2. Moreover, I think that the paper should be divided into two papers, where in one paper the authors would deal with the basic idea and theoretical settings and in the other part of the paper give experimental results that were performed on several different machines? By conducting experiments on a large number of machines, the authors obviously do not have the space to deal in more detail and more clearly present the very interesting basic idea of this valuable work.

Thank you for acknowledging the paper. The core of the paper is how the CPS-PWM changes the high-frequency electromagnetic force order of the multi-phase motor to suppress vibration. All the theoretical analysis serves for the core idea. Considering the theory and experiments in the paper are very closely related, so we decided not to split them into two papers this time.

The paper shows the experiments of three motors to better verify the effectiveness of the proposed method on different motors. Although all three motors

are multi-module motors, Motor1 is interger slot, while Motor2 and Motor3 are fractional slot. There is a difference between the order analysis of the electromagnetic force in the integer slot motor and the fractional slot motor. In the paper, different types of motors are adopted for experiments and the experiments results prove the usability of the vibration reduction method on different motors.

Thanks very much for your comments and suggestions. In our future work about vibration suppression of motors, which would be more complicated than this idea in this paper, we would try to give theoretical analysis, experimental results and discussions in two papers.

3. In addition to the above, I believe that the paper can be written much more literately - the paper should be read and the way of writing should be corrected by someone whose English is natural language?

Thanks for your reminding. We have reduced the use of long sentences in the revised manuscript to make it easier to read. Grammatical errors and inaccurate words have also been corrected. At the same time, we adjusted the structure of the paper to make it easier to understand.